International Journal of Mechanical, Industrial and Aerospace Sciences
ISSN: 2517-9950
Vol:4, No:2, 2010

Enhanced Efficacy of Kinetic Power Transform for High-Speed Wind Field

Nan-Chyuan Tsai, Chao-Wen Chiang, and Bai-Lu Wang

***Abstract*—**The three-time-scale plant model of a wind power generator, including a wind turbine, a flexible vertical shaft, a Variable Inertia Flywheel (VIF) module, an Active Magnetic Bearing (AMB) unit and the applied wind sequence, is constructed. In order to make the wind power generator be still able to operate as the spindle speed exceeds its rated speed, the VIF is equipped so that the spindle speed can be appropriately slowed down once any stronger wind field is exerted. To prevent any potential damage due to collision by shaft against conventional bearings, the AMB unit is proposed to regulate the shaft position deviation. By singular perturbation order-reduction technique, a lower-order plant model can be established for the synthesis of feedback controller. Two major system parameter uncertainties, an additive uncertainty and a multiplicative uncertainty, are constituted by the wind turbine and the VIF respectively. Frequency Shaping Sliding Mode Control (FSSMC) loop is proposed to account for these uncertainties and suppress the unmodeled higher-order plant dynamics. At last, the efficacy of the FSSMC is verified by intensive computer and experimental simulations for regulation on position deviation of the shaft and counter-balance of unpredictable wind disturbance.

***Keywords*—**Sliding Mode Control, Singular Perturbation, Variable Inertia Flywheel.

I. Introduction

DUE to limited petroleum storage underground, the problem of energy crisis is getting more and more serious so that the development of new energy or new energy storage methods becomes urgent and significant. Besides, to prevent air pollution and environmental deterioration resulting from burning fossil fuels, any type of clean and renewable energy is intensively desired. Wind power is one of the promising energy sources. Wind turbines were popularly equipped to convert wind power to kinetic energy. The main stream of wind turbine studies is to obtain maximum kinetic power at low maintenance cost. However, how to ensure safe operation for wide range of wind speed has not been much addressed. Due to the wind speed being unpredictable, the conventional bearings for wind power generators may be damaged by any unexpected causes. More seriously, the entire wind power generator, whose cost might be 3M USD or even higher, can be severely wrecked or even burned up.

Nan-Chyuan Tsai is with the Department of Mechanical Engineering, National Cheng Kung University, No. 1, University Road, Tainan 70101, Taiwan (phone: 886-6-2757575 ext. 62137; fax: 886-6-2369567; e-mail: nortren@mail.ncku.edu.tw).

Chao-Wen Chiang is with the Department of Mechanical Engineering, National Cheng Kung University (e-mail: n1894127@mail.ncku.edu.tw).

Bai-Lu Wang is with the Chung-Shan Institute of Science & Technology, Taoyuan County, Taiwan (e-mail: csist@csistdup.org.tw).

II. Dynamics of Wind Power Generator

The configuration of the studied vertical wind power system is shown in Fig. 1, where the Z-axis denotes the vertical direction. That is, a VAWT (Vertical Axis Wind Turbine) is considered in this work. An Active Magnetic Bearing (AMB) unit is employed to replace the conventional bearing set such that the lateral position deviation of the shaft of wind turbine can be regulated via feedback control loop. In addition, the wind turbine is equipped with a set of Variable Inertia Flywheel (VIF) which is shown in Fig. 2. Once the maximum allowable rotational speed of wind turbine is reached or even exceeded, the rotational speed of wind turbine is automatically regulated to retain at the rated rotational speed by VIF. That is, by activation of VIF the wind turbines can operate even in strong wind field.

A. Characteristics of Wind Turbine

The aerodynamics and mechanics of the wind turbine is studied at first. The thrust force and aerodynamic torque exerting on the blades of wind turbine are dependent of the applied wind speed. Hence, a wind speed model has to be constructed to describe the pattern of the possible wind excitation.

1. Wind Speed Model

The wind speed is the key factor as to the induced power by wind turbine. For simplicity, the wind speed model can be constructed by the linear combination of base wind (V_{WB}), gust wind (V_{WG}), ramp wind (V_{WR}) and noise wind (V_{WN}) [1]. The wind speed model then can be simply expressed as follows:

$$V_W = \overline{V}_W + \delta V_W \tag{1a}$$

$$\overline{V}_W = V_{WB} \tag{1b}$$

$$\delta V_W = \varpi_1 V_{WG} + \varpi_2 V_{WR} + \varpi_3 V_{WN} \tag{1c}$$

where the weighting factors, ϖ_1, ϖ_2 and ϖ_3, are uncertain but their variation intervals can be estimated.

2. Power Output of Wind Turbine

The power output of wind turbine depends on the wind speed, tip-speed ratio (i.e., the ratio of the speed at blade tip to the applied wind speed), pitch angle of blades and the aerodynamic torque. How the aerodynamic torque exerting on the blades in details can be referred to [2]. For a wind turbine

with the wind speed model, similarly the power can be stated as:

$$P_w(V_W) = \frac{1}{2}\rho V_W^3 \pi R_r^2 \quad (2)$$

where R_r is the length of blade. In realistic application, however, the blades can only preserve "partial" wind power, by power coefficient, C_P, that is,

$$P_r(V_W) = \frac{1}{2} C_P \rho V_W^3 \pi R_r^2 \quad (3)$$

where $C_P = 4\kappa(\cos\xi - \kappa)^2$ represents the fraction of the transmitted power through the cross-sectional area, A_b, based on which the turbine converts it into electric power. κ is the axial flow induction factor and ξ is the yaw of the rotor. The fraction factor C_P is decreased as the yaw is increased, as shown in Fig. 3. It is noted that the maximum value of C_P is about 59.3% [3], which is the so-called Betz limit. Under absence of wind wake or swirl, the thrust force exerting on the blades can then be approximated by:

$$F_r(V_W) = \frac{3}{4}\pi \cos(\xi) C_P \rho V_W^2 R_r^2 \quad (4)$$

Therefore, the aerodynamic torque exerting on the blades can then be approximated by:

$$\Gamma_r(V_W) = \frac{C_P \rho V_W^3 \pi R_r^2}{2\dot{\theta}} \quad (5)$$

where $\dot{\theta}$ is the rotation speed of the shaft.

B. Modeling of Rotor/AMB System with VIF

1. Dynamics of Variable Inertia Flywheel

The schematic diagram of Variable Inertia Flywheel (VIF) is depicted in Fig. 2. There are four identical mass-spring modules which are placed by ninety degrees orderly. Because of the centrifugal force, the steel beads are moved rapidly away from the shaft once a certain level of torque or above is applied. That is, the inertia of the VIF is variable and depends on the distance between the shaft and the stretched steel beads.

By Newton's 2nd Law, the equations of motion of VIF can be described as follows:

$$m_b \ddot{\beta} + c_\beta \dot{\beta} + (k_S - m_b \dot{\theta}^2)\beta = 0 \quad (6a)$$

$$(I_d + I_b + 4m_b \beta^2)\ddot{\theta} + (c_\theta + 8m_b \beta \dot{\beta})\dot{\theta} = \Gamma_r(V_W) \quad (6b)$$

where β is the distance of the steel beads apart away from the shaft (or rotor), m_b the mass of each the steel bead, c_β the translational viscous damping between steel bead and its track, k_S the spring constant, θ the spin angle of the shaft, I_d the polar mass moment of inertia of shaft, I_b the overall polar mass moment of inertia of blades, c_θ the rotational viscous damping against the rotation of shaft and Γ_r the aerodynamic torque which exerts on the blades.

2. Equations of Motion for Rotor/AMB

The dimensions and coordinate for the rotor are defined in Fig. 4. The element of the rotor, to be analyzed by FEM (Finite Element Method), consists of two nodes. Each node has four degrees of freedom. In this paper, the thrust force exerting on the blades, shown in Fig. 5, is referred to and named as the *follower force* hereafter. In order to simplify the mathematic model of the entire wind power generator, the blades of turbine are assumed as rigid and the rotor is regarded as a lumped-mass system so that the controller synthesis in Section III can be simplified. By inclusion of the turbine, the equations of motion of the shaft can be constructed in finite element sense as follows:

$$M\ \ddot{q} - \Delta_D(\dot{\theta})\, G\, \dot{q} + [K - \Delta_K(V_W)]\, q = 0 \quad (7)$$

where $q = [V_1 \ \ W_1 \ \ B_1 \ \ \Gamma_1 \ \cdots \ V_n \ \ W_n \ \ B_n \ \ \Gamma_n]^T$ is the displacement vector of the shaft and turbine set and $n = 1, 2, \cdots, 7$. M, G and K are the structural mass matrix, gyroscopic damping matrix and system stiffness matrix respectively, (in details can be referred to [4]). Δ_D and Δ_K are the parameters uncertainties of the gyroscopic damping matrix and system stiffness matrix respectively. Δ_D, the multiplicative uncertainty, is resulted from the rotational speed of the shaft, $\dot{\theta}(V_W)$. Δ_K, the additive uncertainty, is resulted from the follower force, i.e., F_r (more details can be referred in [4]).

The position deviation of the shaft is to be regulated by the Active Magnetic Bearing (AMB) unit in this work. By ignoring the magnetic flux leakage, hysteresis and fringing effect, the dynamics of each electromagnet in AMB can be described as:

$$L^d \frac{d i_d}{dt} + R^d i_d + K_{emf}^d \dot{q}_d = e_d \quad (8a)$$

$$F_m^d = K_m^d \left(\frac{i_d}{q_d}\right)^2 \quad (8b)$$

where the subscript, $d = x$ or y, denotes the electromagnet pair of AMB in X-direction or in Y-direction respectively. L^d is the inductance of the wound coil, R^d the resistance of the coil, K_{emf}^d the coefficient of electromotive force, i_d the coil current, e_d the applied voltage, F_m^d the induced magnetic force, K_m^d the coefficient of the electromagnetic force and q_d the air gap. By taking Taylor's expansion at the equilibrium and assuming the EM (Electromagnetic) poles are identical and therefore the subscript "d" is dropped hereafter, the linearized magnetic force can be obtained in matrix-vector form as follows:

$$F_m = K_D\, q + K_I\, i \quad (9)$$

where K_D and K_I are the force-displacement stiffness matrix and force-current stiffness matrix respectively. i is the coil current in vector form, i.e., $i^T = [i_x \ \ i_y]$. It is noted that since the magnetic bearing inherently possesses negative force-displacement stiffness so that the eigenvalues of the symmetric matrix K_D are all negative. From Eq. (7) and Eq. (9), the equations of motion of the rotor/AMB system can be obtained as follows:

$$M\ \ddot{q} - \Delta_D(\dot{\theta})\, D\, \dot{q} + [K - K_D - \Delta_K(V_W)]\, q = K_I\, i \quad (10a)$$

$$L\dot{i} + R\,i + K_{emf}\,\dot{q} = e \tag{10b}$$

where

$$L = diag(L^x, L^y) \tag{10c}$$

$$R = diag(R^x, R^y) \tag{10d}$$

$$K_{emf} = \begin{bmatrix} 0_{2\times 20} & \vdots & K_{emf}^x & 0 & \vdots & 0_{2\times 6} \\ & \vdots & 0 & K_{emf}^y & \vdots & \end{bmatrix} \tag{10e}$$

$$e^T = [e_x \quad e_y] \tag{10f}$$

It is noted that from the second term of LHS of Eq. (10a), the damping coefficient of the rotor system is time-variant with respect to the rotation speed of shaft, which is partially governed by VIF. The overall stiffness of the rotor/AMB system is decreased by the wind speed, i.e., Δ_K, but increased by the magnetic (negative) force-displacement stiffness, K_D. The state-space representation of the rotor/bearing system can be described as follows:

$$\dot{X} = A_X X + B_X u \tag{11}$$

where

$$X = [q \quad \dot{q} \quad i]^T \tag{12a}$$

$$\mathrm{A}_X = \begin{bmatrix} 0 & I & 0 \\ -M^{-1}[K - K_D - \Delta_K(V_W)] & \Delta_D(V_W)\,M^{-1}G & M^{-1}K_I \\ 0 & -L^{-1}K_{emf} & -L^{-1}R \end{bmatrix} \tag{12b}$$

$$B_X = \begin{bmatrix} 0 & 0 & L^{-1} \end{bmatrix}^T \tag{12c}$$

$$u = e \tag{12d}$$

where the system matrix, i.e., A_X, is Linear Parameter Variant (LPV) with respect to the wind speed, V_W. That is, the system matrix A_X can be further divided into two components, $\overline{A}_X(\overline{V}_W)$ and $\delta A_X(\overline{V}_W, \delta V_W)$. The nominal system matrix $\overline{A}_X$ is defined by setting the wind speed, V_W, to be its nominal value, $\overline{V}_W$. $\delta A_X(\overline{V}_W, \delta V_W)$ is defined as: $\delta A_X(\overline{V}_W, \delta V_W) = A_X - \overline{A}_X(\overline{V}_W)$.

3. Model Reduction by Singular Perturbation

In this work, the slow subsystem consists of primary modes, i.e., the first two natural modes of mechanical subsystem. The residual modes, i.e., the third and higher modes of mechanical subsystem, are regarded as the fast subsystem. It is well-known that the response caused by the higher modes is much faster than that by primary modes. Numerically, the physical value of the inductance of the coil at AMB is much smaller than any other system parameters. The eigenvalues of the nominal open-loop system are shown in Fig. 6. It is observed from Fig. 6 that the eigenvalues of the nominal open-loop system can be clustered into three groups, i.e., the eigenvalues of harmonic mechanical subsystem, electric subsystem and higher-order mechanical subsystem. In another words, the rotor/AMB system processes three-time-scale property. By singular perturbation technique [5], the reduced-order models, i.e., the harmonic mechanical subsystem, electric subsystem and higher-order mechanical subsystem and defined as slow subsystem, intermediate subsystem and fast subsystem respectively, can be obtained.

III. Frequency Shaping Sliding Mode Control

In this section, Frequency Shaping Sliding Mode Control (FSSMC) is synthesized for the rotor/AMB system. The post-filter dynamics and sliding surface can be described as follows [6]:

$$\dot{\varsigma} = F_f\,\varsigma + \overline{G}\,X \tag{13a}$$

$$S_s = \overline{K}\,X + K_2\,\varsigma \tag{13b}$$

where $\overline{K}$, $\hat{G}$, K_a and $\hat{K}$ are designed based on linear quadratic approach. Let $S_s = \dot{S}_s = 0$, which are the so called sliding conditions, then the equivalent control of FSSMC for the rotor/AMB system can be obtained:

$$u_{eq} = -(\overline{K}\,B_X)^{-1}[(\overline{K}\,\overline{A}_X + K_2\overline{G})\,X + K_2\,F_f\,\varsigma] \tag{14}$$

where $\overline{K}$ is designed such that $\overline{K}\,B_X$ is nonsingular. On the other hand, the nonlinear switch control of FSSMC is synthesized to satisfy the associated reaching condition, and can be developed as follows:

$$u_n = -(\overline{K}\,B_X)^{-1}[(|\,\overline{K}\,|U|\,X\,| + N_s)\,Sgn(S_s)] \tag{15}$$

where $N_s > 0$ and U is the upper bound for system matrix uncertainties, i.e., $|\,\delta A_X\,| \le U$.

IV. Simulation Results and Discussions

The test rig of the proposed wind power generator is shown in Fig. set 7. It is assumed that the profile of the wind speed to exert on the wind turbine is shown in Fig. 8. It is noted that the simulations are undertaken by personal computer, interface module ***DS1104*** by *dSPACE* and the environment by *Matlab* simulink. The rotational speed of the shaft and the position of the steel beads are accordingly altered due to the aerodynamic torque by wind turbine and shown in Fig. 9. The rated speed of wind turbine is set as 500 RPM. From Fig. 9, once the rotational speed of shaft exceeds 500 RPM, the steel beads are automatically stretched out, and the rotational speed of shaft is showed down and retained at 500 RPM until the strong wind sequence passes by. In another words, the VIF is successful to be applied for the wind speed higher than the rated speed. Since the rotation speed of shaft is limited by VIF, the possibility of potential damage of blades and bearing sets is greatly reduced.

The physical values of parameters of the rotor/AMB system are summarized and listed in Table I. The aerodynamic torque exerted on the blades can be regarded as the multiplicative uncertainty upon viscous damping coefficient. On the other

hand, the effect of the thrust force by wind can be regarded as the additive uncertainty upon system stiffness. Therefore, a SMC (Sliding Mode Control) loop is proposed to account for these uncertainties. However, since the shaft is assumed to be flexible, the higher-order modes (i.e., 3rd-order and higher) and the boundary layer dynamics of the mechatronic system constitute the unmodeled dynamics. In order not to excite the high-frequency modes of the wind power system, a low pass filter is additionally included to incorporate with the SMC. Assume the system parameters variation, i.e., $\text{norm}(\delta A_x)/\text{norm}(\overline{A}_x) \approx 20\%$, then the associated follower force and the shaft speed are shown in Fig. 10. In order to inspect the equivalent stiffness and the equivalent time constant, the free response of the closed-loop system under FSSMC is shown in Fig. 11. By intensive experimental simulations, it is verified that the FSSMC exhibits superior disturbance rejection capability to account for unpredictable wind excitation.

TABLE I
PHYSICAL PARAMETERS VALUES FOR WIND TURBINE

Young's Modulus	$7\times10^{10}\ Kg/m^2$
Mass Density	$2700\ Kg/m^3$
Transverse Shear Form Factor	0.9
Shear Modulus	$2.6\times10^{10}\ Kg/m^2$
Total Length of Shaft	$0.48\ m$
Total Mass of Blades	$2.4\ Kg$
Radius of Blades	$1\ m$
Mass of Steal Bead	$0.1\ Kg$
Stiffness of VIF	$1\times10^5\ N/m$

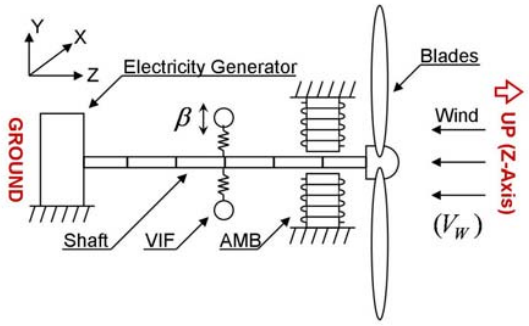

Fig. 1 Schematic Diagram of Wind Power System

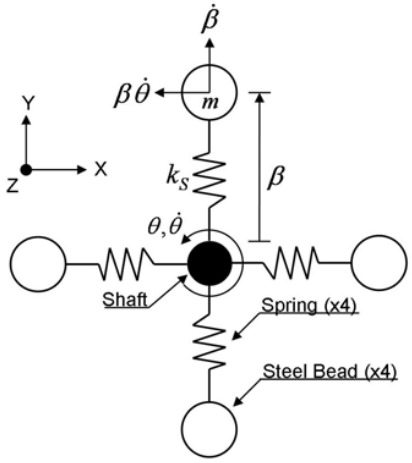

Fig. 2 Schematic Diagram of Variable Inertia Flywheel

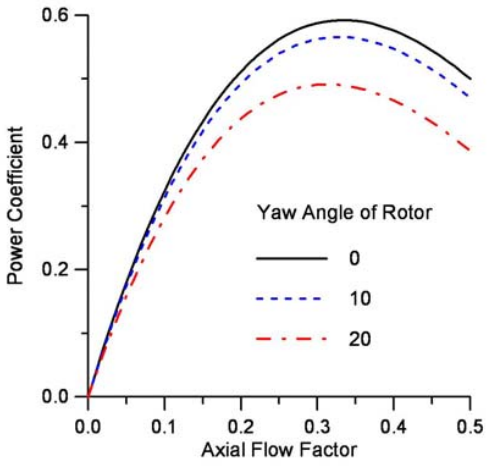

Fig. 3 Effect on Power Coefficient by Yaw Angle and Axial Flow Factor

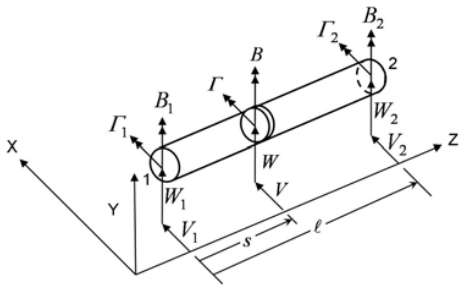

Fig. 4 Finite Elements for Shaft

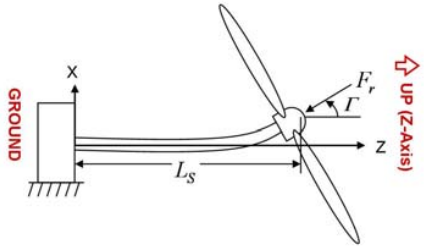

Fig. 5 Follower Force Exerting on Blades

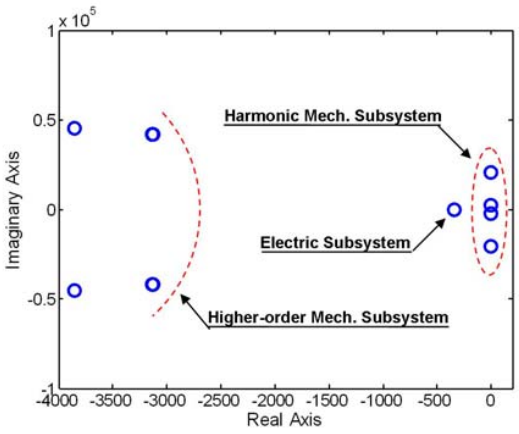

Fig. 6 Groups of Eigenvalues of Open-loop System

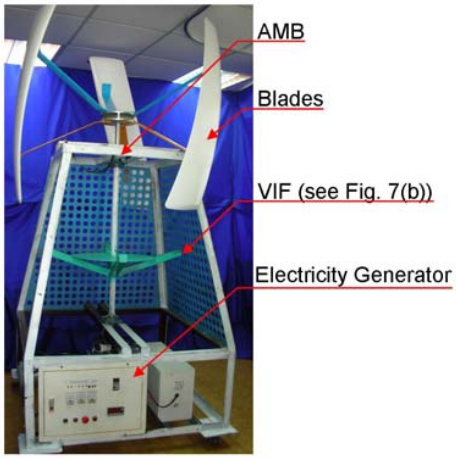

Fig. 7(a) Test Rig of Wind Power Generator

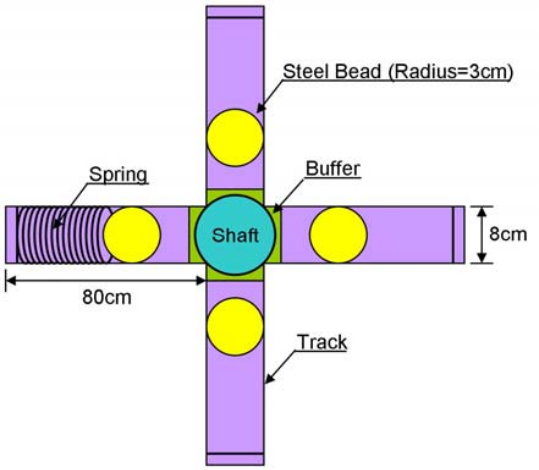

Fig. 7(b) Top View of the VIF

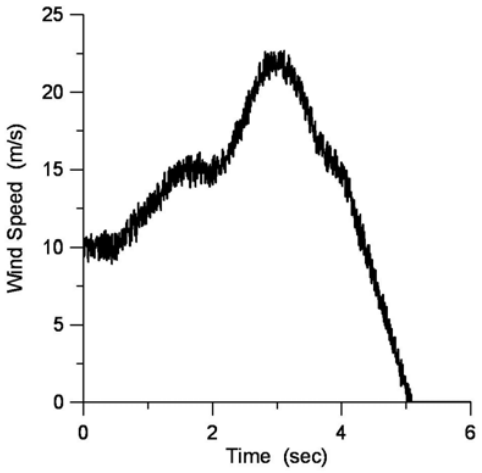

Fig. 8 Applied Wind Speed by Wind

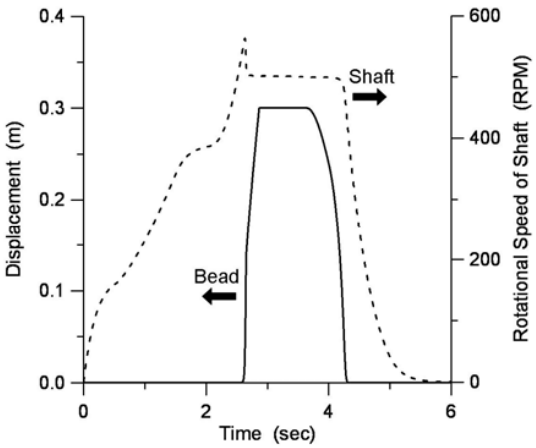

Fig. 9 Steel Beads Stretched by Strong Wind

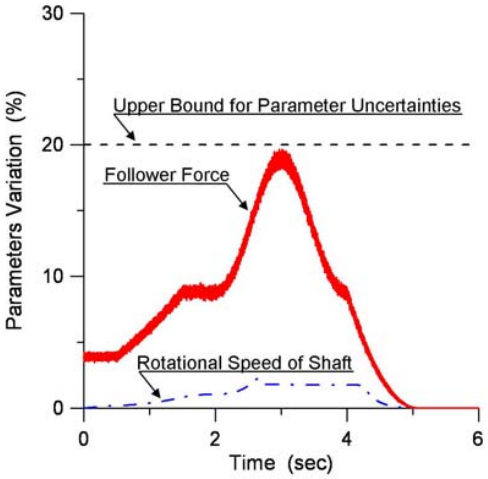

Fig. 10 Parameters Variation under Variable Wind Speed

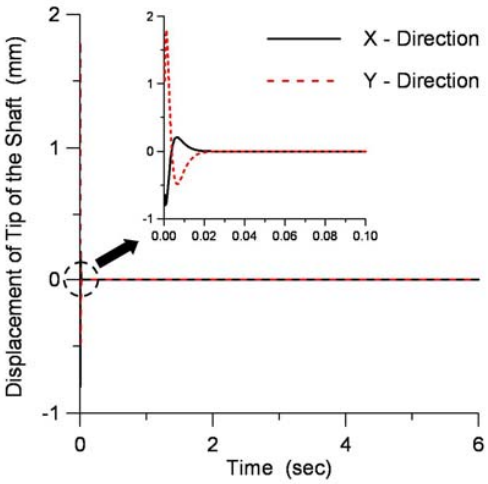

Fig. 11 Free Response of the Closed-loop System under FSSMC

V. Conclusion

The Frequency Shaping Sliding Mode Control (FSSMC) loop is synthesized to account for position deviation of the spindle used for wind power generator. In order to make the wind power generator still operate as the spindle speed exceeds its rated speed, a Variable Inertia Flywheel (VIF) is equipped so that the spindle speed can be slowed down if any stronger wind is applied. To prevent potential damage due to collision of shaft against bearings, an Active Magnetic Bearing (AMB) unit is proposed to regulate the shaft position deviation, in addition to the VIF module. However, the integrated system, including AMB unit, shaft and VIF module, becomes a three-time-scale plant model due to the time constant of the electrical subsystem much smaller than ones of mechanical subsystem and high-order dynamics of the flexible shaft. Since the electrical inductance at AMB unit and the residual modes in the rotor/VIF mechanical subsystem play crucial roles for studied wind power system, they can be modeled as the singular perturbation parameters. By singular perturbation order-reduction technique, the reduced-order model can be constructed for the synthesis of feedback controller. On the other hand, the unmodeled higher-order dynamics can be regarded as one of the uncertainties of the plant model. Besides, two major system parameter uncertainties, i.e., the additive uncertainty and multiplicative uncertainty, are constituted by the follower force and VIF respectively. The upper bound of system parameters variation can be therefore estimated for the basis of FSSMC synthesis. At last, the efficacy of the FSSMC is verified by intensive computer and experimental simulations. By assuming a compound wind sequence, including the step and ramp types, is applied, the capability of FSSMC is inspected, both for regulation on position deviation of the shaft and counter-balance of unpredictable wind disturbance.

Acknowledgment

The authors would like to express their appreciations for equipment access and technical support from Chung-Shan Institute of Science & Technology with CSIST-954-V103 (99).

References

[1] D.-J. Lee, L. Wang, Small-signal stability analysis of an autonomous hybrid renewable energy power generation/energy storage system part I: Time-domain simulations, IEEE Transactions on Energy Conversion 23 (908) 311-320.
[2] J. F. Manwell, J. G. McGowan, A. L. Rogers, Wind Energy Explained: Theory, Design and Application. Chichester, UK, Wiley, 2002.
[3] B. E. Muhando, T. Senjyu, A. Yona, H. Kinjo, T. Funabashi, Regulation of WTG dynamic response to parameter variations of analytic wind stochasticity, Wind Energy 11 (908) 133-150.
[4] L. W. Chen, D.-M. Ku, Finite element analysis of natural whirl speeds of rotating shafts, Computers and Structures 40 (891) 741-747.
[5] K.-K. D. Young, P. V. Kokotovic, V. I. Utkin, Singular Perturbation Analysis of High-gain Feedback Systems, IEEE Transactions on Automatic Control 22 (897) 931-938.
[6] A. J. Koshkouei, A. S. I. Zinober, Robust frequency shaping sliding mode control, in: IEE Proceedings: Control Theory and Applications, Vol. 147, 2000, pp. 312-320.